THE JOURNAL OF PHYSICAL CHEMISTRY C

Article

Cite This: J. Phys. Chem. C 2019, 123, 8902−8907

pubs.acs.org/JPCC

Incommensurate Quantum Size Oscillations of Oligoacene Wires Adsorbed on Au(111)

Michiel J. van Setten,[†,‡] Dimitra Xenioti,[§] Mébarek Alouani,[§] Ferdinand Evers,[∥] and Richard Korytár*[,⊥]

[†]Nanoscopic Physics, Institute of Condensed Matter and Nanosciences, Université catholique de Louvain, 1348 Louvain-la-Neuve, Belgium

[‡]IMEC, Kapeldreef 75, 3001 Leuven, Belgium

[§]Institut de Physique et Chimie des Matériaux de Strasbourg, UMR 7504 CNRS-UdS, 23, Rue du Loess, BP 43, 67034 Strasbourg, Cedex 2, France

[∥]Institut I - Theoretische Physik, Universität Regensburg, Universitätsstraß e 31, 93053 Regensburg, Germany

[⊥]Department of Condensed Matter Physics, Faculty of Mathematics and Physics, Charles University, 121 16 Prague, Czech Republic

Supporting Information

ABSTRACT: Acenes have attracted interest for a long time partly because of their electronic structure and partly because they are expected to show interesting correlation effects. For the isolated molecules, our recent theoretical work suggests a possibility for oscillations of the excitation gaps with the length of the molecule. In view of the recent experimental progress of on-surface synthesis, we employ the density functional theory to investigate here the fate of these oscillations for oligoacenes adsorbed on a Au(111) surface. We show that the surface perturbs the oligoacene gaps seen in isolation only weakly, implying that incommensurate oscillations survive. Effects beyond the density functional description (correlations, charging effects) are discussed.

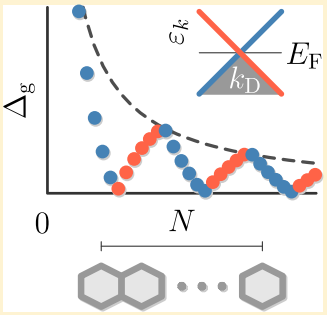

INTRODUCTION

Oligoacenes (Oac) have been considered a central element of the design of molecular interfaces because their excitation gap can be controlled by tuning the molecule's length, i.e., the number of fused benzene rings, N.[1,2] Apart from this technological motivation, there is also a profound fundamental interest in them because they are expected to exhibit unusual electronic properties, such as antiferromagnetic (polyradical) correlations[3−6] or gap oscillations with length.[7] These properties will become most apparent in longer molecules. Therefore, it is encouraging that in most recent experiments Oac of unprecedented lengths, N = 10, 11, have been synthesized and investigated.[8−10]

For the Oac on a metallic substrate, the electron−electron interaction is expected to be significantly screened. In this case, an interacting Hubbard-type Hamiltonian is expected to provide an adequate effective description of the ground-state and low-energy excitations. A numerically exact calculation based on the density-matrix renormalization group (DMRG) theory predicts a singlet ground state for the Oac-Hubbard model.[11] Moreover, Schmitteckert et al. predict that the length dependence of the optical gap, $\Delta_g(N)$, exhibits incommensurate size oscillations (IO). This effect can be understood as relict[7] of the band structure of polyacene (Pac),[12,13] i.e., the limit $N \to \infty$, as illustrated in Figure 1.

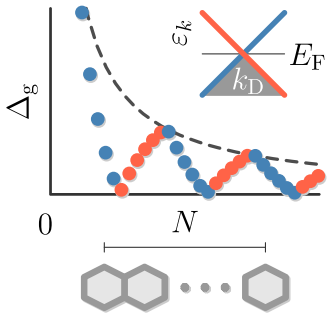

Figure 1. Evolution of the highest occupied molecular orbital/lowest unoccupied molecular orbital (HOMO/LUMO) gap, Δ_g, of oligoacenes with the increasing number of rings, N, exhibiting incommensurate oscillations (colored dots). Oscillations can be understood as deriving from a crossing of valence and conduction band of polyacene at an incommensurate wavenumber, $k_D \approx 0.9\pi/a$, a denoting the lattice constant (inset). Colors differentiate parity of energy bands of the highest occupied molecular orbital. For illustration, a $1/N$ envelope (dashed line) is also shown that represents conventional "particle in a box" scaling.

Received: December 20, 2018
Revised: February 19, 2019
Published: March 8, 2019

DOI: 10.1021/acs.jpcc.8b12213
J. Phys. Chem. C 2019, 123, 8902−8907

So far, systematic ab initio studies of the length dependence have focused on isolated molecules.[5,6,14−17] In the present work, we investigate the length dependence of the excitation gaps in the case when the molecules physisorb on a metallic substrate. Due to screening mediated by the substrate, one expects that correlation effects are reduced, especially those related to the long-range nature of the Coulomb interaction. We calculate the band structure of Pac adsorbed on Au(111) by density functional theory (DFT). Our data suggests that the band crossing of Pac is preserved. To provide further evidence, we study the adsorption of individual Oac, tetracene ($C_{18}H_{12}$), pentacene ($C_{22}H_{14}$), hexacene ($C_{26}H_{16}$), and heptacene ($C_{30}H_{18}$), on Au(111). We extrapolate the adsorbate's HOMO/LUMO gaps as a function of length, finding evidence for the gap minimum. Thus, the Pac band structure and the gaps of Oac support the IO on Au(111).

Our study is furthermore stimulated by the recent progress in on-surface synthesis of Oac.[8,9,18−20] The advantage of the on-surface approach is that the molecules are stabilized and the HOMO/LUMO gaps of individual adsorbates can be determined by means of scanning tunneling spectroscopy. In particular, Zuzak et al.[19] have investigated the length dependence of the Oac on Au(111) (up to undecacene). A comparison of their results and our prediction is given in the Discussion section.

COMPUTATIONAL DETAILS

The adsorption is treated using DFT in the Kohn−Sham formalism. We employed a projector augmented plane-wave basis set[21] with an energy cutoff of 400 eV using the VASP package[22] and the PBE functional.[23] van der Waals (vdW) interactions between the molecules and the surface were included using the semiempirical DFT-D3 method,[24] proposed by Grimme et al.[25] The gold surface is approximated by a slab of four atomic layers and a vacuum region of 20 Å thickness.

Polyacene on Au(111). Our aim is to inspect the impact of the gold surface on the conduction and valence bands of Pac. Therefore, we consider a periodic unrelaxed geometry, whose construction is described below. Relaxation effects are taken into account later in the next section.

The construction of a supercell for Pac (a periodic analogue of linear Oac) lying on Au(111) presents a technical difficulty due to the mismatch of the lattice constants of Au(111) and Pac. We overcome this challenge by a significant modification of −9 and +7% in the lattice constants of Au and Pac, respectively, leading to the smallest supercell containing a single Pac unit cell, a half-ring C_4H_2 (see the inset of Figure 2). While this calculation will not properly reproduce certain details, such as the charging of the molecule, it nevertheless is informative with respect to the degree of hybridization between molecular and substrate orbitals. It is indicative of the stability of the band structure with respect to the substrate contact.

With the above-mentioned lattice modification, the Pac is placed parallel to the metallic surface and its axis is aligned with the $\langle 01\bar{1}\rangle$ direction. The distance between the Pac plane and the topmost layer of Au is fixed at 2.8 Å, comparable to the adsorption distances obtained for relaxed Oac.

Oligoacenes on Au(111). We use the same surface slab dimensions for all four molecules (10 × 4); see Scheme 1. To sample the surface Brillouin zone, a mesh of 3 × 5 × 1 k-points was used, providing a k-point density comparable to those employed previously on similar systems.[26,27]

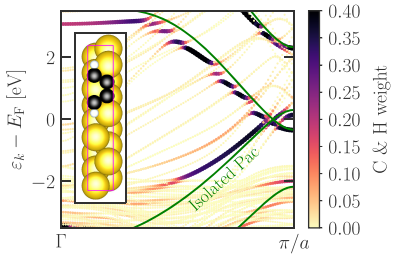

Figure 2. Band structure of Pac on Au(111) from the slab geometry (see the inset, the red rectangle delineates the unit cell). The color of each dot represents the sum of the squares of the wave function amplitudes on all C and H basis orbitals, indicating the molecular contribution (weight) in the wave function. For comparison, band energies of isolated Pac are also shown (green line).

Scheme 1. Unit Cell of the Slab Geometry Underlying the DFT Calculation for Heptacene on Au(111)[a]

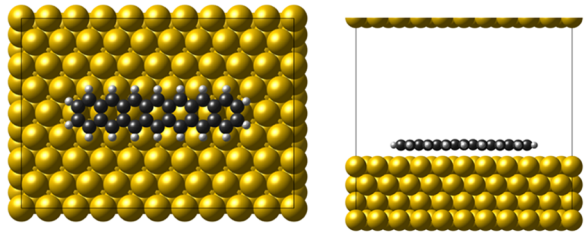

[a]Top view (left) and side view (right).

We obtained the adsorption geometry by optimizing the atomic coordinates of the molecules and the top two layers of the gold slab. The atomic positions of the bottom two layers are kept frozen. For the relaxed structures, the absolute values of the total forces acting on the molecule are less than 0.05 eV/Å and the total energy difference between the last relaxation step is less than 10^{-3} eV. The adsorption energies are defined as

$$E_{ad} = E(C_{4N+2}H_{2N+4}/Au) - E(C_{4N+2}H_{2N+4}) - E(Au) \quad (1)$$

where $E(C_{4N+2}H_{2N+4}/Au)$ is the total energy of the adsorbed system, $E(C_{4N+2}H_{2N+4})$ is the total energy of the isolated molecule, and $E(Au)$ is the total energy of the clean Au(111) surface (per slab cell).

For comparison, we also introduce a reference system, consisting of a molecule in its isolated geometry kept fixed at the distance of 6.5 Å parallel to the surface. The molecules in the reference system have negligible interaction with Au.

RESULTS

Band Structure of Pac on Au(111). Figure 2 shows the band structure calculated from the Γ point toward the corner of the Brillouin zone along the wire's axis. The isolated Pac has four π bands in the energy window given in the plot. As one also infers from Figure 2, these bands clearly reflect in the electronic structure after deposition of the molecule to the substrate. In particular, as in the isolated case, there is a band inversion at $k = k_D = 0.893\pi/a$ and a concomitant band crossing. Remarkably, we do not detect a tendency for a significant gap opening in the crossing. This property does not depend on the choice of the supercell, as long as the reflection symmetry (see the inset of Figure 2) is preserved.[12] The wavenumber of the "Dirac point", k_D, and the Fermi velocity,

DOI: 10.1021/acs.jpcc.8b12213
J. Phys. Chem. C 2019, 123, 8902−8907

v_F, are reduced by 2 and 8%, respectively, from the values of isolated Pac. These shifts are an artifact of the compactified unit cell, and as we shall demonstrate below, the actual renormalization of k_D and v_F is very small.

In Figure 2, the Pac conduction (LUMO) band is seen to exhibit a handful of avoided crossings with the sp bands of gold. The crossings merely reflect the finite size of the slab. In the thermodynamic limit, the Pac bands acquire a continuous broadening. In the Supporting Information, we estimate the broadening (half-width) of the conduction band to be roughly 40 meV. This estimate is much smaller than the size of the Pac band gap at the corner of the Brillouin zone (630 meV). In conclusion, the band-structure calculation indicates that the structure of Pac bands near the Fermi level is only weakly affected by the substrate.

Oac on Au(111). *Structural Properties.* For pentacene, our results confirm earlier experimental and theoretical findings: the center of the molecule is located at an hcp hollow site with the long molecular axis aligned with the close-packing direction $\langle 01\bar{1}\rangle$.[28,29] We find that tetracene, hexacene, and heptacene align in a similar way.

Table 1 shows a survey of the binding distances and energies. The central finding is that the average adsorption distance and the E_{ad}/x saturate with the increasing Oac length. The adsorption distances and E_{ad} are typical for physisorption. Concerning absolute numbers, it is known that E_{ad} depends significantly on the underlying exchange−correlation functional. Toyoda et al. observe changes of 25% for $C_{22}H_{14}$ upon changing the vdW flavor.[28] In our DFT-D3 calculations, we find the E_{ad} of $C_{22}H_{14}$ in between the values calculated by Toyoda and co-workers.

Table 1. Binding Distances[a]

molecule	$C_{18}H_{12}$	$C_{22}H_{14}$	$C_{26}H_{16}$	$C_{30}H_{18}$
N	4	5	6	7
z(Au) [Å]	0.01	0.02	0.02	0.02
z(C)	2.92	2.94	2.93	2.94
z(C-Au)	2.91	2.92	2.92	2.92
$-E_{ad}/x$ [meV]	109.3	108.4	94.3	103.0

[a] z(Au) and z(C) are the average z-coordinates of the topmost Au atoms and carbons; the reference point $z = 0$ is the coordinate of the unreconstructed topmost Au layer. z(C-Au) is the (average) vertical distance between the reconstructed topmost layer of Au and the carbons. The final row contains adsorption energies per carbon atom ($x = 4N + 2$).

In pentacene and heptacene, we observe a slight bending of the molecule toward the substrate; the middle ring drops about 0.1 Å with respect to the outer rings. A similar protrusion has been observed experimentally for heptacene on Ag(111)[18] and for pentacene on Cu(111).[30] However, the bending that we calculate on Au(111) is noticeably weaker than that on the other two noble metals. Anthracene remains flat within a tolerance of ±0.01 Å. In hexacene, the carbon atoms joining the outer rings to the second outer rings drop about 0.1 Å. We remark that in longer Oac, further molecular reconstruction can be expected because of incommensurability of Oac and Au lattice parameters. However, the data presented here suggest that the effect of Au will be generally weak.

Projected Density of States. The electronic structure of the adsorbates can be understood by plotting the density of states (DOS) projected on the carbon atoms (Figure 3). The DOS of the reference systems (also shown in Figure 3) displays resonances near the Fermi level, which can be unambiguously connected to the frontier orbitals, HOMO and LUMO. Moreover, employing a constant energy shift, the resonances of the reference systems match the spectrum of the adsorbed molecules. In this way, the HOMO and LUMO resonances can be identified. We define the molecular orbital energy, ε_{HOMO}, ε_{LUMO}, as the center of the Gaussian fit locally to the DOS peak. The resulting orbital energies and gaps, $\Delta_g^{Au} := \varepsilon_{LUMO} - \varepsilon_{HOMO}$, are given in Table 2.

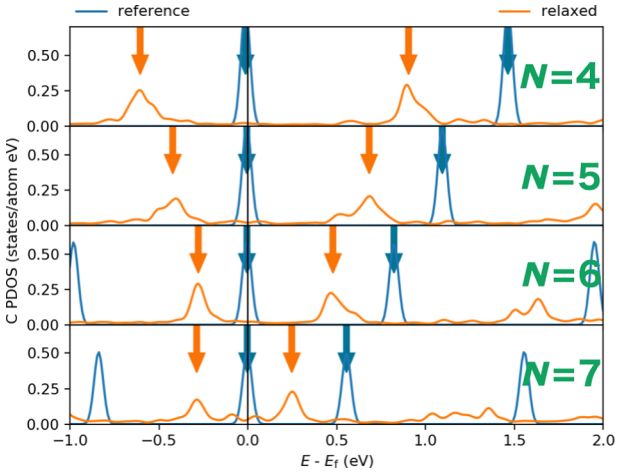

Figure 3. Evolution of the density of states projected on the C atoms with the increasing length, N (top to bottom: tetracene, pentacene, hexacene, and heptacene). Orange: DOS for adsorbed molecules as shown in Scheme 1 for hexacene. Blue: reference calculation for the same geometry except lifting the molecule 6 Å away from the substrate. Arrows indicate HOMO and LUMO resonances. The spectra involve Gaussian smearing of 60 meV.

Table 2. Center Positions of the HOMO and LUMO Resonances Extracted for the Adsorbed Molecule from Figure 3[a]

N	molecule	ε_{HOMO}	ε_{LUMO}	Δ_g^{Au}	Δ_g^{is}
4	$C_{18}H_{12}$	−0.6068	0.9040	1.511	1.623
5	$C_{22}H_{14}$	−0.4227	0.6818	1.105	1.142
6	$C_{26}H_{16}$	−0.2792	0.4779	0.757	0.797
7	$C_{30}H_{18}$	−0.2880	0.2469	0.534	0.540

[a] The third column gives the Kohn−Sham gap of adsorbed molecules, $\Delta_g^{Au} = \varepsilon_{LUMO} - \varepsilon_{HOMO}$. For comparison, the last column presents the Kohn−Sham gaps, Δ_g^{is}, of isolated molecules.[7] The unit of energy is eV.

We plot the dependence of Δ_g^{Au} on the inverse length, $1/N$, in Figure 4 along with the gaps of isolated Oac, Δ_g^{is}. The gaps of the adsorbed Oac follow closely the trend of the isolated molecules, which in turn follow zone-folding of the Pac band structure. From zone-folding arguments of ref 7, it follows that the HOMO/LUMO gaps depend linearly on $N/(N + 1)$, namely

$$\Delta_g(N) = 2v_F\left(-\frac{N}{N+1}\cdot\frac{\pi}{a} + k_D\right) \quad (2)$$

$$\text{for } N < N_1 = \frac{ak_D}{\pi - ak_D} \quad (3)$$

DOI: 10.1021/acs.jpcc.8b12213
J. Phys. Chem. C 2019, 123, 8902−8907

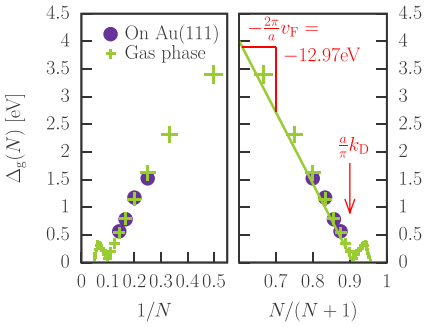

Figure 4. Comparison of the HOMO/LUMO gaps of Oac (N = 4, 5, 6, 7) adsorbed on Au(111) (purple dots) and isolated (N = 2, ..., 20, green crosses). The data for isolated molecules are taken from ref 7. In the left panel, the gaps are plotted conventionally as a function of $1/N$. When the gaps are plotted against $N/(N + 1)$, zone-folding arguments predict that the gaps lie on a straight line, whose slope is given by $-\frac{2\pi}{a}v_F$ and intersecting the abscissa at $\frac{a}{\pi}k_D$. The straight line is parameterized by v_F and k_D from the isolated Pac.

The parameters are Fermi velocity, v_F, wavenumber of the "Dirac point", k_D, and lattice parameter (length of the acene hexagon), a. The variable $N/(N + 1) \times \pi/a$ represents the wavenumber of the HOMO/LUMO pair. The factor 2 arises because we subtract the conductance and valence band energies. The expression is valid until the first gap minimum is reached at $N = N_1$. Inspired by the latter analytical form, we plot the computed gaps of adsorbed molecules as a function of $N/(N + 1)$ in Figure 4 and compare them with the isolated systems. As it is expected already from Table 2, the gaps of the adsorbates lie almost on a straight line, similarly to the isolated molecules. Notice that the value 1 of the abscissa corresponds to the infinite limit. Hence, the negative slope clearly indicates the tendency to close the gap at finite N. By comparing the left and right panels of Figure 4, it can be seen that the change of the independent variable from $1/N$ to $N/(N + 1)$ removes a slight bending of the gap trace, apparent at smaller N.

For comparison, in the right panel of Figure 4 (straight line), we also plot the analytical expression (2) with parameters $\frac{\pi}{a}v_F = 6.485$ eV and $\frac{a}{\pi}k_D = 0.9102$ taken from the isolated Pac band structure (ref 7). As demonstrated in the latter reference, a small increase of Δ_g^{is} above the analytical zone-folding expression is due to static structural relaxation effects. Remarkably, the deviation of Δ_g^{Au} from the analytical expression is of the same order as the deviation of Δ_g^{is}. We conclude that the surface-induced renormalization of v_F and k_D, seen in the Kohn–Sham spectrum, is very small. The Kohn–Sham spectrum does not include renormalization due to surface-driven electron–electron interaction effects, e.g., screening. These effects can affect the gaps quantitatively but will not change the oscillatory nature of $\Delta_g^{Au}(N)$, as long as the metallicity of the adsorbed Pac is preserved.

In summary, our analysis indicates that the Kohn–Sham gaps of acenes on Au(111) follow from the zone-folding rules, as for the isolated molecules. Deviations from the zone-folding predictions (apart from small-size effects) appear as a weak scatter (Figure 4). The causes of the scatter are, e.g., (1) the level spacing of the artificial slab and (2) the incommensurate potential of the surface. Consequently, our results provide evidence for the oscillatory nature of Oac gaps, $\Delta_g^{Au}(N)$, within the Kohn–Sham framework. In principle, the reconstruction due to incommensurability of Pac and Oac lattices can provide matrix elements that couple the conduction and valence bands, opening a gap Δ_{dis} at k_D. However, the data presented here suggest that the effect of Au is generally weak. Thus, the gap Δ_{dis} will not affect the IO until $\Delta_g^{Au}(N)$ falls below Δ_{dis}.

DISCUSSION

In this section, we discuss effects that are not included in the DFT description, namely, electronic correlations and charging energies. Finally, we analyze a recent scanning tunneling spectroscopy of Oac on Au(111).

Correlation Effects. The gaps shown in Figure 4 (both adsorbed and isolated Oac) tend to zero with the increasing N, in accordance with the metallicity of the Pac, resulting from closed-shell DFT with semilocal functionals. It has been established in several quantum chemistry studies[3−5] that isolated Oac have a strongly correlated electronic ground state, resulting in (possibly) gapped electronic excitations for $N \to \infty$. Thus, it is unclear whether the band-structure effect of the IO can be revealed in optical spectra of the isolated Oac.[10] Schmitteckert et al.[11] investigated correlation effects resulting from repulsive short-ranged (screened) interactions by employing a tight-binding model with a Hubbard term. Their main finding is that the IO are robust even for moderate interaction strengths,[31] despite a small correlation gap. Thus, correlations resulting from a short-range interaction are weak in the sense that they do not destroy the band-structure effects (IO).

In the context of the previous discussion, it is plausible that the PBE-DFT electronic structure is much more realistic for Oac on Au than it is for isolated molecules. The surface screens electron–electron interaction; thus, correlation effects tend to get weaker. Naturally, this tendency is not reflected in the comparison of the gaps Δ_g^{is} and Δ_g^{Au} in Figure 4 because the PBE-DFT correlation is already weak in isolated Oac. The agreement between Δ_g^{is} and Δ_g^{Au} is indicative of the weak metal–molecule interaction, which implies only small geometric distortions, negligible charge transfer, and weak hybridization.

Charge Gaps. We briefly relate our results to the recent STM experiment on acenes on Au(111) surfaces.[9] As a preparation, we recall that such measurements result in a determination of the charge gap, $\Delta_c(N)$ (fundamental gap), which is not actually obtained in our DFT calculations. The computational difficulty is related to the absence of the derivative discontinuity in most available approximations of exchange–correlation functionals.[32]

The charge gap comprises two contributions, one that is reflecting quantum confinement and the other one reflecting the charging energy, $E_c(N)$.

$$\Delta_c(N) = 2v_F\left(-\frac{N}{N+1}\cdot\frac{\pi}{a} + k_D\right) + E_c(N), \quad (N \le N_1) \tag{4}$$

The first term takes a form specific for acenes and has been derived in our previous work.[7] The origin of the charging energy, $E_c(N)$, is straightforward to understand in closed isolated systems, where it accounts for the energy difference between the LUMO of the uncharged system and the HOMO of the same system with a single excess charge.

For generic isolated molecular wires with N repetitive units, we estimate $E_c(N) \propto \log(N)/N$. The $\log(N)$ term reflects the long-range nature of the Coulomb interaction. Thus, it is present as long as self-screening can be neglected. The $\log(N)$

DOI: 10.1021/acs.jpcc.8b12213
J. Phys. Chem. C 2019, 123, 8902−8907

dependence implies that the charging energy dominates the charge gap of finite-size isolated metallic wires in the large N limit.

On metallic substrates, the wire's molecular orbitals can hybridize with surface states. As we have seen for the case of acenes on Au(111), the hybridization can be weak so that the molecular orbitals keep their character. In this situation, the observable reflecting the charge gap is the projected local density of states (spectral function) with its HOMO- and LUMO-derived excitation peaks. In this case, the Coulomb interaction is screened, so the logarithmic prefactor in the surface analogue of $E_c(N)$ does not arise and the overall magnitude of $E_c(N)$ will be significantly weakened.[33−35] Overall, one expects that the IO will survive in $\Delta_c(N)$; however, they are weaker in the sense that the gap may not fully close at the minimum N_1 anymore.[36]

Discussion of the Experiment. In their recent study, Zuzak and co-workers observe a monotonously decreasing charge gap obtained by scanning tunneling spectroscopy.[9] In Figure 5, we have reproduced their published experimental

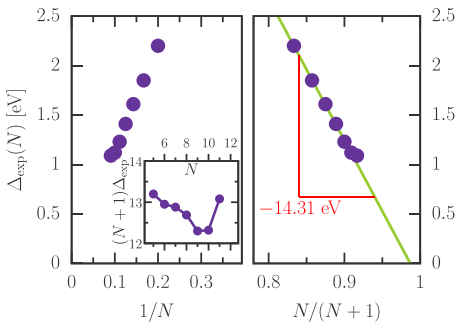

Figure 5. Experimental charge gaps, $\Delta_{exp}(N)$, from ref 9 shown as purple dots. The gaps are plotted as a function of $1/N$ (left panel) and $N/(N+1)$ (right panel). The inset in the left panel shows $(N+1)\Delta_{exp}$. The green line is a least-square fit of $\Delta_{exp}(N)$ to the linear function of $N/(N+1)$. In analogy with Figure 4, we also indicate the slope of the line, which is in good agreement with the theoretical Fermi velocity of polyacene. The longest available Oac ($N = 11$) was excluded from the fit.

data, $\Delta_{exp}(N)$, in a way motivated by the plotting of our theory data seen in Figure 4.[37] The left panel of the figure displays the experimental gap, $\Delta_{exp}(N)$, as a function of $1/N$. Similar to Figure 4, the data falls approximately onto a line. Compared to the DFT, the experimental line appears to have undergone a vertical shift of ≈1 eV. We propose that this shift could be related to charging effects not contained in the theory, as discussed in the previous section. The experimental length dependence of the gaps is not oscillatory in the set of Oac experimentally available. However, the theory predicts the gap minimum to occur at $N = 10$. Hence, an upturn occurs at $N = 11$. The experimental data have a kink at $N = 11$, which is easily revealed when $(N+1)\Delta_{exp}$ is plotted in the inset of Figure 5, as in ref 11. Moreover, interactions with the surface can induce a small shift of the upturn point, of the order of one ring. Apparently, despite the experiment being already close, definite conclusions about IO might require slightly longer molecules and very well defined error bars.

In the right panel of Figure 5, we also show the experimental data plotted in the same way as in Figure 4, right side. Additionally, we show a linear fit of the data points. The abscissa is proportional to the wavenumber. However, we emphasize that the intersection of the line with the abscissa in Figure 5 does not imply the first gap minimum because of charging effects. Remarkably, the value of the slope turns to be similar to the DFT value, as indicated in the figure. In view of eq 4, the slope involves a contribution from $E_c(N)$. A future theoretical work can elaborate on the length dependence of charging energies, $E_c(N)$, in a more quantitative way. The linear Oac are ideal benchmark systems, as they offer means to compare trends of the excitation gaps, instead of the gaps of various individual systems.

CONCLUSIONS

We have addressed the length dependence of the excitation gaps of oligoacenes (Oac) adsorbed on the surface of Au(111) by density functional theory (DFT) with a PBE functional and a D3 dispersion correction. For tetracene, pentacene, hexacene, and heptacene ($N = 4, 5, 6, 7$), our structural analysis confirms earlier findings that the Oac weakly physisorb on Au(111).[28,38,39] The calculations show that the gaps of adsorbates, $\Delta_g^{Au}(N)$, differ only by small amount (<7%) from the gaps of isolated Oac, $\Delta_g^{is}(N)$, reflecting the weak physisorption. Since for longer N the gaps $\Delta_g^{is}(N)$ show incommensurate oscillations[7] (IO), we conclude that the DFT gaps $\Delta_g^{Au}(N)$ will show IO as well. In particular, $\Delta_g^{Au}(N)$ will have a first upturn at N around 11 ± 1.

For isolated Oac, the metallic-like behavior of $\Delta_g^{is}(N)$, as seen in closed-shell DFT, is disputed due to strong correlations originating from long-range Coulomb interaction between electrons.[5,10] On the other hand, a metallic surface causes screening of the Coulomb interaction. It was found in a previous study that correlations due to screened interaction do not destroy the oscillations.[11] Combining the latter result with the electronic structure from DFT, we conclude that the incommensurate oscillations of Oac on Au(111) will be revealed experimentally by optical or electronic transport probes. The experimental observation of the first upturn of $\Delta_g^{Au}(N)$ requires molecules of lengths up to $N \approx 13$ rings.

ASSOCIATED CONTENT

Supporting Information

The Supporting Information is available free of charge on the ACS Publications website at DOI: 10.1021/acs.jpcc.8b12213.

Golden rule calculation of the band broadening to make a quantitative estimate of the band broadening using the supercell calculation (PDF)

AUTHOR INFORMATION

Corresponding Author

*E-mail: korytar@karlov.mff.cuni.cz.

ORCID

Richard Korytár: 0000-0003-4949-4147

Notes

The authors declare no competing financial interest.

ACKNOWLEDGMENTS

We acknowledge computational resources from HPC méso centre of Strasbourg and GENCI-CINES grant 2014(2015)-gem1100. R.K. acknowledges the support from the PRIMUS/Sci/09 program of the Charles University.

DOI: 10.1021/acs.jpcc.8b12213
J. Phys. Chem. C 2019, 123, 8902−8907

REFERENCES

(1) Anthony, J. E. Functionalized Acenes and Heteroacenes for Organic Electronics. *Chem. Rev.* **2006**, *106*, 5028−5048.
(2) Roncali, J.; Philippe, L.; Philippe, B. Molecular Materials for Organic Photovoltaics: Small is Beautiful. *Adv. Mater.* **2014**, *26*, 3821−3838.
(3) Bendikov, M.; Duong, H. M.; Starkey, K.; Houk, K.; Carter, E. A.; Wudl, F. Oligoacenes: Theoretical Prediction of Open-shell Singlet Diradical Ground States. *J. Am. Chem. Soc.* **2004**, *126*, 7416−7417.
(4) Hachmann, J.; Dorando, J. J.; Avilés, M.; Chan, G. K.-L. The Radical Character of the Acenes: A Density Matrix Renormalization Group Study. *J. Chem. Phys.* **2007**, *127*, No. 134309.
(5) Bettinger, H. F. Electronic Structure of Higher Acenes and Polyacene: The Perspective Developed by Theoretical Analyses. *Pure Appl. Chem.* **2010**, *82*, 905−915.
(6) Yang, Y.; Davidson, E. R.; Yang, W. Nature of Ground and Electronic Excited States of Higher Acenes. *Proc. Natl. Acad. Sci. USA* **2016**, *113*, E5098−E5107.
(7) Korytár, R.; Xenioti, D.; Schmitteckert, P.; Alouani, M.; Evers, F. Signature of the Dirac Cone in the Properties of Linear Oligoacenes. *Nat. Commun.* **2014**, *5*, No. 5000.
(8) Krüger, J.; García, F.; Eisenhut, F.; Skidin, D.; Alonso, J. M.; Guitián, E.; Pérez, D.; Cuniberti, G.; Moresco, F.; Peña, D. Decacene: On-Surface Generation. *Angew. Chem., Int. Ed.* **2017**, *129*, 12107−12110.
(9) Zuzak, R.; Dorel, R.; Kolmer, M.; Szymonski, M.; Godlewski, S.; Echavarren, A. M. Higher Acenes by On-Surface Dehydrogenation: From Heptacene to Undecacene. *Angew. Chem., Int. Ed.* **2018**, *57*, 10500−10505.
(10) Shen, B.; Tatchen, J.; Sanchez-García, E.; Bettinger, H. F. Evolution of the Optical Gap in the Acene Series: Undecacene. *Angew. Chem., Int. Ed.* **2018**, 10666−10669.
(11) Schmitteckert, P.; Thomale, R.; Korytár, R.; Evers, F. Incommensurate Quantum-size Oscillations in Acene-based Molecular Wires - Effects of Quantum Fluctuations. *J. Chem. Phys.* **2017**, *146*, No. 092320.
(12) Kivelson, S.; Chapman, O. L. Polyacene and a New Class of Quasi-one-dimensional Conductors. *Phys. Rev. B* **1983**, *28*, 7236−7243.
(13) Lowe, J. P.; Kafafi, S. A.; LaFemina, J. P. Qualitative MO Theory of Some Ring and Ladder Polymers. *J. Phys. Chem.* **1986**, *90*, 6602−6610.
(14) Rayne, S.; Forest, K. A Comparison of Density Functional Theory (DFT) Methods for Estimating the Singlet-Triplet (S0-T1) Excitation Energies of Benzene and Polyacenes. *Comput. Theor. Chem.* **2011**, *976*, 105−112.
(15) Wilhelm, J.; Del Ben, M.; Hutter, J. GW in the Gaussian and Plane Waves Scheme with Application to Linear Acenes. *J. Chem. Theory Comput.* **2016**, *12*, 3623−3635.
(16) Rangel, T.; Hamed, S. M.; Bruneval, F.; Neaton, J. B. Evaluating the GW Approximation with CCSD(T) for Charged Excitations Across the Oligoacenes. *J. Chem. Theory Comput.* **2016**, *12*, 2834−2842.
(17) Dupuy, N.; Casula, M. Fate of the Open-shell Singlet Ground State in the Experimentally Accessible Acenes: A Quantum Monte Carlo Study. *J. Chem. Phys.* **2018**, *148*, No. 134112.
(18) Zugermeier, M.; et al. On-surface synthesis of heptacene and its interaction with a metal surface. *Nanoscale* **2017**, *9*, 12461−12469.
(19) Zuzak, R.; Dorel, R.; Krawiec, M.; Such, B.; Kolmer, M.; Szymonski, M.; Echavarren, A. M.; Godlewski, S. Nonacene Generated by On-Surface Dehydrogenation. *ACS Nano* **2017**, *11*, 9321−9329.
(20) Sun, Q.; Zhang, R.; Qiu, J.; Liu, R.; Xu, W. On-Surface Synthesis of Carbon Nanostructures. *Adv. Mater.* **2018**, *30*, No. 1705630.
(21) Blöchl, P. E. Projector Augmented-wave Method. *Phys. Rev. B* **1994**, *50*, 17953−17979.
(22) Kresse, G.; Furthmüller, J. Efficient Iterative Schemes for ab initio Total-energy Calculations Using a Plane-wave Basis Set. *Phys. Rev. B* **1996**, *54*, 11169−1118.
(23) Perdew, J. P.; Burke, K.; Ernzerhof, M. Generalized Gradient Approximation made Simple. *Phys. Rev. Lett.* **1996**, *77*, 3865−3868.
(24) We use the cutoff radii 50 and 20 Å for pair interactions and the coordination number, respectively, and damping parameters corresponding to the PBE functional.
(25) Grimme, S.; Antony, J.; Ehrlich, S.; Krieg, H. A Consistent and Accurate ab initio Parametrization of Density Functional Dispersion Correction (DFT-D) for the 94 Elements H-Pu. *J. Chem. Phys.* **2010**, *132*, No. 154104.
(26) Tonigold, K.; Groß, A. Adsorption of Small Aromatic Molecules on the (111) Surfaces of Noble Metals: A Density Functional Theory Study with Semiempirical Corrections for Dispersion Effects. *J. Chem. Phys.* **2010**, *132*, No. 224701.
(27) Da Silva, J. L. F.; Stampfl, C.; Scheffler, M. Converged properties of clean metal surfaces by all-electron first-principles calculations. *Surf. Sci.* **2006**, *600*, 703−715.
(28) Toyoda, K.; Hamada, I.; Lee, K.; Yanagisawa, S.; Morikawa, Y. Density Functional Theoretical Study of Pentacene/Noble Metal Interfaces with van der Waals Corrections: Vacuum Level Shifts and Electronic Structures. *J. Chem. Phys.* **2010**, *132*, No. 134703.
(29) France, C.; Schroeder, P.; Forsythe, J.; Parkinson, B. Scanning Tunneling Microscopy Study of the Coverage-dependent Structures of Pentacene on Au (111). *Langmuir* **2003**, *19*, 1274−1281.
(30) Schuler, B.; Liu, W.; Tkatchenko, A.; Moll, N.; Meyer, G.; Mistry, A.; Fox, D.; Gross, L. Adsorption Geometry Determination of Single Molecules by Atomic Force Microscopy. *Phys. Rev. Lett.* **2013**, *111*, No. 106103.
(31) By moderate it is meant that the Hubbard *U* is comparable to the non-interacting band-width.
(32) Perdew, J. P.; Parr, R. G.; Levy, M.; Balduz, J. L. Density-Functional Theory for Fractional Particle Number: Derivative Discontinuities of the Energy. *Phys. Rev. Lett.* **1982**, *49*, 1691−1694.
(33) Neaton, J. B.; Hybertsen, M. S.; Louie, S. G. Renormalization of Molecular Electronic Levels at Metal-Molecule Interfaces. *Phys. Rev. Lett.* **2006**, *97*, No. 216405.
(34) Biller, A.; Tamblyn, I.; Neaton, J. B.; Kronik, L. Electronic Level Alignment at a Metal-Molecule Interface from a Short-Range Hybrid Functional. *J. Chem. Phys.* **2011**, *135*, No. 164706.
(35) Egger, D. A.; Liu, Z.-F.; Neaton, J. B.; Kronik, L. Reliable Energy Level Alignment at Physisorbed Molecule-Metal Interfaces from Density Functional Theory. *Nano Lett.* **2015**, *15*, 2448−2455.
(36) The conclusion is similar to the one obtained for isolated Oac, where the derivative-discontinuity can partially be restored using hybrid exchange-correlation functionals: Korytár et al. analyzed in this way the charged excitations in the isolated Oac by using the hybrid PBE0 functional.[7] They observe IO superimposed on a smooth background associated with the charging energy. We emphasize that this conclusion is based on the assumption that effects of the long-range Coulomb interaction do not invoke a strongly-correlated phase.
(37) Experimental data have been given in ref 9 without error bars, so that they are also missing in Figure 5. The reported values $\Delta_{exp}(N)$ have been obtained from peak positions. As can be seen in the supporting information of ref 9, the corresponding peak width takes very roughly 20% of the peak value.
(38) Liu, W.; Ruiz, V. G.; Zhang, G.-X.; Santra, B.; Ren, X.; Scheffler, M.; Tkatchenko, A. Structure and Energetics of Benzene Adsorbed on Transition-metal Surfaces: Density-functional Theory with van der Waals Interactions Including Collective Substrate Response. *New J. Phys.* **2013**, *15*, No. 053046.
(39) Soe, W.-H.; Manzano, C.; De Sarkar, A.; Chandrasekhar, N.; Joachim, C. Direct Observation of Molecular Orbitals of Pentacene Physisorbed on Au (111) by Scanning Tunneling Microscope. *Phys. Rev. Lett.* **2009**, *102*, No. 176102.

DOI: 10.1021/acs.jpcc.8b12213
J. Phys. Chem. C 2019, 123, 8902−8907